Accepted Manuscript

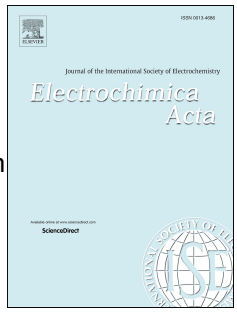

Bis(1,10-phenanthroline) copper complexes with tailored molecular architecture: From electrochemical features to application as redox mediators in dye-sensitized solar cells

Elisabetta Benazzi, Mirko Magni, Alessia Colombo, Claudia Dragonetti, Stefano Caramori, Carlo Alberto Bignozzi, Roberto Grisorio, Gian Paolo Suranna, Maria Pia Cipolla, Michele Manca, Dominique Roberto

PII: S0013-4686(18)30605-4

DOI: 10.1016/j.electacta.2018.03.103

Reference: EA 31469

To appear in: *Electrochimica Acta*

Received Date: 25 January 2018

Revised Date: 15 March 2018

Accepted Date: 17 March 2018

Please cite this article as: E. Benazzi, M. Magni, A. Colombo, C. Dragonetti, S. Caramori, C.A. Bignozzi, R. Grisorio, G.P. Suranna, M.P. Cipolla, M. Manca, D. Roberto, Bis(1,10-phenanthroline) copper complexes with tailored molecular architecture: From electrochemical features to application as redox mediators in dye-sensitized solar cells, *Electrochimica Acta* (2018), doi: 10.1016/j.electacta.2018.03.103.

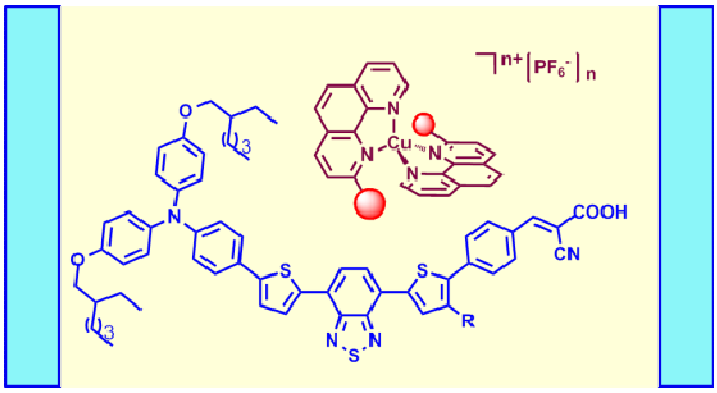

Bis(1,10-phenanthroline) copper complexes with tailored molecular architecture: from electrochemical features to application as redox mediators in dye-sensitized solar cells.

Elisabetta Benazzi,[a] Mirko Magni,[b]* Alessia Colombo,[b]** Claudia Dragonetti,[b] Stefano Caramori,[a] Carlo Alberto Bignozzi,[a] Roberto Grisorio,[c] Gian Paolo Suranna,[c] Maria Pia Cipolla,[d,e] Michele Manca[d]*** and Dominique Roberto[b]

[a] Dipartimento di Scienze Chimiche e Farmaceutiche, Università di Ferrara, Via F. di Mortara, Ferrara, Italy.

[b] Dipartimento di Chimica, Università degli Studi di Milano, UdR dell'INSTM, Via Golgi 19, Milano, Italy.

[c] Dip. di Ingegneria Civile, Ambientale, del Territorio, Edile e di Chimica, Politecnico di Bari, via Orabona, Bari and CNR-NANOTEC c/o Campus Ecotekne, via Monteroni, Lecce, Italy.

[d] Center for Biomolecular Nanotechnology - Fondazione Istituto Italiano di Tecnologia, Via Barsanti 14, Arnesano (Lecce), Italy.

[e] Dipartimento di Ingegneria dell' Innovazione, Università del Salento, Campus Ecotekne, Via per Monteroni, 73100, Lecce, Italy.

Corresponding authors e-mail: *mirko.magni@unimi.it; **alessia.colombo@unimi.it; ***michele.manca@iit.it

Abstract

In the last few years, copper coordination compounds turned out to be effective competitors of cobalt complexes as redox mediators in the formulation of iodine-free electrolytes for dye-sensitized solar cells (DSSCs). However, the lack of a clear correlation between electrochemical

signatures of copper complexes (*i.e.* half-wave potential and heterogeneous electron transfer rate) and photoelectrochemical performance of solar devices makes difficult the optimization of their coordination sphere. Therefore, to partially fill this gap and to elucidate the intrinsic correlation between the molecular architecture of these complexes and their electrochemical features, we prepared four $Cu^{+/2+}$ redox couples in which the copper center is coordinated by two 1,10-phenanthrolines bearing various substituents in position 2. These complexes were well characterized, from both electrochemical and spectroscopic point of view, and tested as electron shuttles in lab-scale photoelectrochemical cells sensitized with two efficient π-extended benzothiadiazole dyes. It appeared that 2-aryl-1,10-phenanthrolines effectively combine suitable optical and electrochemical properties. While a fast electron transfer kinetics generally positively affects the dye regeneration process, an optimal balance between dye regeneration efficiency, mass transport and heterogeneous electron transfer at both the counter electrode and at the TiO_2 interface, must be achieved in order to optimize DSSC performance. Within our series, the top performer was $[Cu(2\text{-tolyl-1,10-phenanthroline})_2]^{+/2+}$ which achieved a relative 20% and 15% improvement in power conversion efficiency (under 100 mW s^{-1} simulated AM 1.5G illumination) with respect to control cells filled with $[Co(bpy)_3]^{2+/3+}$ (bpy=2,2'-bipyridine) and I^-/I_3^- electrolytes, respectively.

Keywords:

homoleptic bis(1,10-phenanthroline) copper complexes; copper redox mediators; iodine-free electrolyte; dye-sensitized solar cells; structure-activity relationship

1. Introduction

Dye-sensitized solar cells (DSSCs), which are composed of mesoporous nanocrystalline TiO_2 layers modified with photosensitizing dyes as photoanodes, redox electrolytes and counter electrodes

(Figure 1), have been actively investigated as photovoltaic devices in alternative to conventional silicon-based inorganic solar cells, because of their potentially low production costs, relatively low toxicity of the constituent elements and relatively high photon-to-current conversion efficiency (PCE) especially under low-light intensities and scattered light conditions [1].

(Figure 1)

DSSCs, easy to fabricate on flexible panels, offer unique transparency and aesthetic advantages with respect to building-integration. However, the promise of DSSCs to become the largest commercially available solar energy conversion technology and the most convenient alternative to silicon is still far to get fulfilled. Among the factors still obstructing the lab-to-market bridge crossing road, there is the failure to achieve DSSCs with long-term stability. Also, further reducing their costs remains an important target as the cost of silicon solar cells has significantly dropped in recent years [2-3].

Since the milestone paper of O'Regan and Grätzel on DSSCs in 1991 [4], photosensitizers have monopolized attention of researchers aimed to maximize their light harnessing, by improving the overlap between the dye absorption spectrum and the solar emission one, and enhance their dipole moment to facilitate the charge separation, by creating suitable conjugated moieties with a donor-π-linker-acceptor architecture [5-10]. For many years, the most efficient DSSCs were based on variously substituted polypyridyl ruthenium complexes as dye and the iodide/triiodide couple (I^-/I_3^-) as electrolyte, reaching PCE around 10-12 % [11-13]. However, in the last decade, the high cost and rarity of ruthenium encouraged the search for efficient noble-metal-free dyes such as organic compounds [5], porphyrins [7], and copper complexes [8-10]. In parallel, an exponential growth of work has been devoted to find alternative redox mediators such as metal transition complexes [14-15] to replace the traditional redox couple I^-/I_3^- which has many problems such as a too negative redox potential, complicated two-electron redox chemistry, corrosiveness and volatility of I_2 in equilibrium with I_3^- complicating long-term cell sealing and therefore hampering long-term stability [16-17]. The use of $Co^{2+/3+}$ complexes as mediators has addressed some of these issues since they

are outer-sphere one-electron redox systems with more positive and tunable redox potentials, affording large V_{oc} [16-17]. In fact, to date record power conversion efficiencies (13-14%) in DSSCs have been reached with a cobalt-based electrolyte in combination with either porphyrins [18-19] or π-delocalized organic dyes [20]. Nevertheless, cobalt complexes have some drawbacks associated with slow mass transport in the electrolyte solution and large internal reorganization energy between the high-spin d^7 and low-spin d^6 states. The limitations caused by the reorganization energy are minimized by using well-designed $Cu^{+/2+}$ complexes with distorted tetragonal geometry [21]. These alternative electron shuttles are of particular interest since copper is a low-cost, environmental friendly metal.

As recently reviewed [10], copper complexes were firstly proposed as electron shuttles in 2005 when, in combination with N719 as dye, $[Cu(2,9\text{-dimethyl-}1,10\text{-phenantholine})_2]^{+/2+}$ reached a PCE of 1.4%, ten-fold higher than that of related $[Cu(1,10\text{-phenantholine})_2]^{+/2+}$, showing the crucial role of the methyl groups in position α to the coordinating nitrogen atoms in order to maintain the distorted tetragonal geometry around the copper center and therefore a very efficient electron transfer process [22]. By using the same redox mediator with various Donor-π-Acceptor organic dyes, there was a progressive growth of PCE from 7% [23] to 8.3 % [24] to 10.3% [25]. Besides, the use of $[Cu(1,1\text{-bis}(2\text{-pyridyl})\text{ethane})_2]^{+/2+}$ [26] and $[Cu(6,6'\text{-dimethyl-}2,2'\text{-bipyridine})_2]^{+/2+}$ [25, 27] redox mediators, in combination with organic dyes, led to PCE of 9.0% and 10.3%, respectively. These copper-based mediators overcame performance of the control cells filled with a reference cobalt-based electrolyte [24, 26,27]. Interestingly, $[Cu(4,4',6,6'\text{-tetramethyl-}2,2'\text{-bipyridine})_2]^{+/2+}$ mediators revealed also very promising for indoor application [28]. Clearly the use of copper-based mediators appears as a key in the fabrication of convenient low-cost DSSCs.

Remarkably, we found that the novel redox couple $[Cu(2\text{-mesityl-}4,7\text{-dimethyl-}1,10\text{-phenantholine})_2]^{+/2+}$ is fascinating as electron shuttle because the presence of the bulky mesityl groups on the phenanthrolines protects as a kiss lock the copper center, leading to slightly superior dye regeneration kinetics and longer electron lifetimes with respect to simpler 2,9-dimethyl-1,10-

phenanthroline based copper complexes [29]. This redox couple allowed to double the efficiency of DSSCs with respect to [Cu(2,9-dimethyl-1,10-phenantholine)$_2$]$^{+/2+}$ in combination with a π-extended benzothiadiazole dye [30] or a ruthenium dye working in the presence of an iron(II) comediator [29]. Also, coupling zinc porphyrin dyes with the related [Cu(2-mesityl-1,10-phenantholine)$_2$]$^{+/2+}$ redox couple afforded efficient DSSCs, exceeding the performance reached by $Co^{2+/3+}$ and I^-/I_3^- reference electrolytes [31].

These observations prompted us to undertake a deeper investigation of the properties of a series of homoleptic copper complexes based on 1,10-phenanthrolines, where the sole 2 position was substituted by various aryl and alkyl moieties. In particular, the electrochemical behavior of copper complexes substituted with mesityl, tolyl, phenyl or *n*-butyl groups (**1/2, 3/4, 5/6, 7/8**, Chart 1) was analyzed and related to the photoelectrochemical characteristics of DSSCs sensitized by π-extended benzothiadiazole dye (**G3** or **G4**, Chart 1) [32,33].

(Chart 1)

2. Experimental

2.1 Synthesis of copper complexes redox mediators (1-8)

2.1.1 General comments

The hindered 2-substituted phenanthroline ligands were prepared by nucleophilic aromatic substitution of the commercially available 1,10-phenanthroline with the suitable lithium derivative. Mesityllithium and tolyllithium were prepared by transmetallation reaction between their bromo-derivative and *tert*-butyllithium in diethylether (Et_2O) as previous described [29] whereas copper complexes **1** and **2**, with 2-mesityl-1,10-phenanthroline as ligand, were synthesized as reported [31].

Solvents for the syntheses were dried by standard procedures: *N,N*-dimethylformamide (DMF) was dried over activated molecular sieves and toluene was distilled over Na/benzophenone. All reagents

were purchased from Sigma-Aldrich and were used without further purification. Reactions requiring anhydrous conditions were performed under argon or nitrogen. Thin layer chromatography (TLC) was carried out with pre-coated Merck F254 silica gel plates. Flash chromatography (FC) was carried out with Macherey-Nagel silica gel 60 (230-400 mesh).

2.1.2 General procedure for Cu(I) complexes

The precursor CuCl was dissolved under argon in acetonitrile and added dropwise to a stirred solution of the suitable 2-substituted-1,10-phenanthroline in dry acetonitrile. The red solution was stirred at room temperature for *ca.* 40 minutes. The solvent was eliminated under reduced pressure and the solid was dissolved in the minimum amount of a mixture H_2O/EtOH. After addition of an aqueous solution of $NaPF_6$, a red precipitate was formed and, after 2 hours, filtered off, washed with H_2O and Et_2O and finally dried under vacuum.

2.1.2.1 [Cu(2-tolyl-1,10-phenanthroline)$_2$]PF_6 (3)

It was obtained starting from CuCl (12.4 mg, 0.126 mmol) in 1.8 mL of acetonitrile and 2-tolyl-1,10-phenanthroline (69.8 mg, 0.258 mmol) in 9.5 mL of acetonitrile. The product was dissolved in a mixture H_2O/EtOH 1/1 (v/v) (*ca.* 10 mL) and $NaPF_6$ (63mg in 2mL of water) was added. The pure product was obtained as a dark red powder in 70% yield.

^{1}H-NMR (400 MHz, CD_2Cl_2) δ 8.93 (d, J =4.39 Hz, 2H), 8.55-8.51 (m, 4H) 8.10(d, J =8.78 Hz, 2H), 8.01 (d, J =8.78 Hz, 2H), 7.88 (dd, J =8.10, 4.3 Hz, 2H), 7.74 (d, J =8.16 Hz, 2H), 6.56 (d, J =7.40 Hz, 2H), 6.42 (t, J =7.39 Hz, 2H), 6.35 (d, J =7.49 Hz, 2H), 6.06 (t, J =7.39 Hz, 2H), 1.85(s, 6H). ^{13}C-NMR (100 MHz, CD_2Cl_2) δ 157.92, 148.63, 143.61, 143.07, 139.70, 136.58, 134.67, 129.42, 128.7, 127.76, 127.64, 126.56, 126.62, 125.14, 123.90, 19.98. Elemental analysis: Calcd. (%) for $C_{38}H_{28}CuF_6N_4P$: C 60.92; H 3.77; N 7.48; found: C 61.01; H, 3.77; N 7.47. MS (FAB$^+$) m/z: 603.13 Found: 603.

2.1.2.2 [Cu(2-phenyl-1,10-phenanthroline)$_2$]PF$_6$ (5)

It was obtained starting from CuCl (19.9 mg, 0.201 mmol) in 2.7 mL of acetonitrile and 2-phenyl-1,10-phenanthroline (106 mg, 0.413 mmol) in 15. mL of acetonitrile. The product was dissolved in a mixture H_2O/EtOH 1/1 (v/v) (*ca.* 15 mL) and $NaPF_6$ (101 mg in 4 mL of water) was added. The pure product was obtained as a dark red powder in 88% yield.

^{1}H-NMR (400 MHz, CD_2Cl_2) δ 9.06 (dd, J =4.3 Hz, J= 1.4 Hz 2H), 8.65 (d, J =8.45 Hz, 2H), 8.47 (d, J =8.45 Hz, 2H), 8.09 (d, J =8.08 Hz, 2H), 8.04 (d, J =8.08 Hz, 2H), 7.96 (dd, J =8.0, 1.4 Hz, 2H), 7.85 (d, J =8.08 Hz, 2H), 7.23 (d, J =7.4 Hz, 4H), 6.66 (t, J =7.4 Hz, 2H), 6.38 (t, J =7.4 Hz, 4H). ^{13}C-NMR (400 MHz; CD_3CN): δ 158.20, 148.83, 143.71, 143.13, 138.68, 136.64, 134.77, 129.40, 128.55, 127.76, 127.68, 126.59, 125.66, 125.14, 124.01. Elemental analysis: Calcd. (%) for $C_{36}H_{24}CuF_6N_4P$ (721.11): C, 59.96; H, 3.35; N, 7.77; found: C, 60.03; H, 3.34; N, 7.80. MS (ESI$^+$) m/z: 575.13 Found: 575.49.

2.1.2.3 [Cu(2-*n*-butyl-1,10-phenanthroline)$_2$]PF$_6$ (7)

It was obtained starting from CuCl (70 mg, 0.366 mmol) in 8 mL of acetonitrile and 2-*n*-butyl-1,10-phenanthroline (300 mg, 1.27 mmol) in 13.3 mL of dry acetonitrile. The solid was dissolved in a mixture H_2O/EtOH 1/2 (v/v) (*ca.* 50 mL) and $NaPF_6$ (305 mg in 9 mL of water) was added. The pure product was obtained as a dark orange powder in 87% yield.

^{1}H-NMR (400 MHz; MeOD): δ 9.06 (d, J=4.1 Hz, 2H), 8.79 (d, J=7.8 Hz, 2H), 8.69 (d, J=8.3 Hz, 2H), 8.23 (d, J=9.0 Hz, 2H), 8.20 (d, J=9.0 Hz, 2H), 8.00 (dd, J_1=7.8 Hz, J_2=4.1 Hz, 2H), 7.93 (d, J=8.3 Hz, 2H), 2.78-2.64 (m, 4H), 1.48-1.22 (m, 4H), 0.69-0.48 (m, 4H), 0.22 (t, J=7.4 Hz, 6H). Elemental Analysis: Calcd. for $C_{32}H_{32}CuF_6N_4P$: C 56.43, H 4.74, N 8.40. Found. C 56.55, H 4.75, N 8.23. MS (ESI$^+$) m/z: 535.19 Found: 535.57.

2.1.3 General procedure for Cu(II) complexes

The phenanthroline ligand was dissolved in acetonitrile and a solution of $CuSO_4*5H_2O$ in water was slowly added. The light green mixture was stirred at room temperature for 1h and then it was concentrated at reduced pressure at about 2 mL and a water solution of $NaPF_6$ was added. The resulting solution was stirred for 2h and then the green precipitate was filtered, washed successively with H_2O and Et_2O and finally dried under reduced pressure.

2.1.3.1 [Cu(2-tolyl-1,10-phenanthroline)$_2$](PF$_6$)$_2$ (4)

Obtained starting from 2-tolyl-1,10-phenanthroline (31.0 mg, 0.114 mmol) in acetonitrile (9 mL) and $CuSO_4*5H_2O$ (14.2 mg, 0.057 mmol) in 2 mL of water. After addition of $NaPF_6$ (40 mg in 1 mL of water), the product was obtained as a green solid in 40% yield.

Elemental Analysis: Calcd. for $C_{38}H_{28}CuF_{12}N_4P_2$: C 51.04, H 3.16, N 6.27. Found. C 51.25, H 3.17, N 6.30. MS (FAB^+) m/z: 603.

2.1.3.2 [Cu(2-phenyl-1,10-phenanthroline)$_2$](PF$_6$)$_2$ (6)

Obtained starting from 2-phenyl-1,10-phenanthroline (30 mg, 0.111 mmol) in acetonitrile (8 mL) and $CuSO_4*5H_2O$ (17.5 mg, 0.07 mmol) in 1.5 mL of water. After addition of $NaPF_6$ (56 mg in 1 mL of water), the product was obtained as a green solid in 68% yield.

Elemental Analysis: Calcd. for $C_{36}H_{24}CuF_{12}N_4P_2$: C 49.92, H 2.79, N 6.47. Found. C 49.97, H 2.81, N 6.46. MS (ESI^+) m/z: 575.42.

2.1.3.3 [Cu(2-*n*-butyl-1,10-phenanthroline)$_2$](PF$_6$)$_2$ (8)

Obtained starting from 2-*n*-butyl-1,10-phenanthroline (38.0 mg, 0.161 mmol) in acetonitrile (3 mL) and $CuSO_4*5H_2O$ (20 mg, 0.08 mmol) in 2 mL of water. After addition of $NaPF_6$ (58 mg in 1 mL of water), the product was obtained as a green solid in 70% yield.

Elemental Analysis: Calcd. for $C_{32}H_{32}CuF_{12}N_4P_2$: C 46.53, H 3.90, N 6.78. Found. C 46.61, H 3.92, N 6.80. MS (ESI^+) m/z: 535.45.

2.2 Electrochemical characterization

Cyclic voltammetry, CV, and electrochemical impedance spectroscopy, EIS, for the electrochemical characterization of copper complexes were performed in a customized three-electrode minicell filled with 2-3 mL of a solution of acetonitrile as solvent with 0.1 M tetrabutylammonium hexafluorophosphate, [TBA]PF_6 as supporting electrolyte. The working solution was well deareated by bubbling nitrogen before starting each measurement. A nitrogen blanket was maintained over the solution during the scans as well. Teflon-embedded glassy carbon electrode GC (geometric surface area 0.071 cm^2) were used as working electrode in combination with a platinum wire as counter electrode and a saturated calomel electrode, SCE, as reference one. To avoid water and chloride leakage into the working solution, SCE was inserted into a glass jacket ending with a porous frit and filled with the same blank electrolytic solution (*i.e.* solvent and supporting electrolyte). The recorded potentials were subsequently referred to the intersolvental reference redox couple $Fc^+|Fc$ (ferricenium|ferrocene) added as external standard (*ca.* $1 \cdot 10^{-3}$ M) at the end of each daily measure. The measures were performed with a potentiostat/galvanostat PGSTAT302N (Metrohm Autolab, The Netherlands) controlled by a PC through GPES and NOVA 1.10 software, equipped with a frequency response analyzer module (FRA2) for EIS measurements. Staircase CV were performed at different sweep potentials (0.02-2 V s^{-1}) with a potential step of 0.001-0.002 V. An instrumental compensation of the resistance (*i.e.* positive feedback) was carefully performed in order to minimize the ohmic drop between the working and reference electrode. EIS spectra were recorded superimposing to a continuous potential bias set at the half-wave potential, $E_{1/2}$, of the analyzed compound a sinusoidal alternating potential signal of 0.01 V amplitude and frequency ranging from $1 \cdot 10^5$ to $1 \cdot 10^{-1}$ Hz. Sixty logarithmically distributed single sine frequencies were employed for recording each spectrum. NOVA 1.10 software was used to validate EIS data (through Kronig-Kramers analysis) and to fit them with a Randles-type equivalent circuit to estimate the charge transfer resistance, R_{ct}, at the electrolyte/electrode interface.

2.3 Dye solar cells fabrication and photoelectrochemical characterization

FTO-coated glass substrates (15 Ω sq^{-1}, purchased from XIN YAN TECHNOLOGY LTD) were cleaned in a detergent solution for 15 min and then in ethanol for 30 min using an ultrasonic bath. Mesoporous TiO_2 electrodes were prepared by doctor blading a commercial paste, namely Dyesol 30NRD up, and subjecting them to thermal sintering at 450 °C for 40 min. The average thickness of the electrodes used in the reported batch of devices was 12 μm. After this first thermal sintering, all the samples were treated with a 40 mM aqueous solution of $TiCl_4$ for 30 min at 70° C, rinsed again with water and ethanol and then subjected to a second sintering process at 500°C for 30 min. After cooling the mesoporous electrodes were immersed into the dye solution (**G3** or **G4**, 0.2 mM) along with chenodeoxycholic acid (30 or 10 mM, respectively) in tetrahydrofuran for 8 h. The counter electrodes were prepared by sputtering a 50 nm Pt layer on a hole-drilled cleaned FTO plate. The two electrodes were then assembled together in a sandwich configuration and sealed upon heating a thermoplastic gasket made of a hot-melt ionomer-class resin (Surlyn 50-μm thickness). The electrolytic solution was injected through the hole on the counter electrode glass. For symmetrical cells, two identical Pt-coated FTO plates were assembled, using a 100-μm thick gasket. Photocurrent *versus* voltage, *j-E*, measurements were performed using a Keithley unit (Model 2400 Source Meter), while a Newport Sol3A Class AAA Solar Simulator (Model 94063A equipped with a 1000W xenon arc lamp) served as a light source, scanning potential from open-circuit to short circuit conditions. The light intensity (or radiant power) was calibrated to 100 mW cm^{-2} using as reference a Silicon standard solar cell. Electrochemical analyses (on both DSSCs and symmetrical cells) were performed using an Autolab PGSTAT 302N, and digitally processed using the NOVA 1.10 software. EIS spectra were recorded by sweeping the frequency from 50 kHz to 0.01 Hz with a logarithmic distribution, using a 10 mV amplitude sine wave potential modulation superimposed to the bias potentials. EIS data were fitted to the equivalent circuit using the ZWiew® software.

2.4 Transient absorption spectroscopy measurements

Transient absorption spectroscopy, TAS, was carried out by a previously described apparatus [34] using the 532 nm harmonic of a nanosecond Nd:YAG laser (Continuum Surelite II). A typical pulse energy of 2 mJ cm^{-2} was used. A 532 nm notch filter prevented laser light from reaching the photomultiplier. Formation of the photo-oxidized dye was probed at 770 nm, by using the monochromatic output of an Applied Photophysics f: 3.4 monochromator coupled to a pulsed Xe arc lamp. Typically 30 laser shots, at a frequency of 0.2 Hz, were averaged to reach a good S/N ratio.

Photoanodes were prepared by a standard procedure. FTO glass plates were washed in 2-propanol for 10 min using an ultrasonic bath, then were heated at 450°C for 20 minutes. A compact TiO_2 blocking underlayer was prepared by spin-coating a 0,3 M titanium(IV) isopropoxide solution in 1-butanol (1000 rpm for 10 s, 2000 rpm for 20 s). Then the substrates were heated up at 500 °C for 15 min. The photoelectrodes were prepared by doctor blading, using a transparent TiO_2 paste (Dyesol 18NR-T). The coated films were heated to 500 °C for 10 min with programmed temperature ramping. After sintering, the electrodes were treated with 0.4 M $TiCl_4$ overnight and heated again at 450° for 30 minutes. Once cooled, the electrodes were dipped for 15 minutes in a 0.2 mM solution of the dye (**G3**) in tetrahydrofuran, containing chenodeoxycholic acid 30 mM.

TAS measurements on transparent thin films in the presence of the electron donor species in acetonitrile were performed by drawing the electrolyte by capillarity inside the chamber (ca. 6−8 μm), constituted by a glass slide pressed against the TiO_2 photoanode. Thus, the negligible optical path allowed to avoid interferences originated by the mediators' absorbance.

Regeneration efficiency was calculated by applying the formula [35]:

$$\eta = \frac{k_{reg}^{'}}{k_{reg}^{'} + k_{rec}} \quad (1)$$

where the pseudo first order recombination, k_{rec}, and regeneration, k'_{reg}, rate constants were obtained by fitting the experimental decay curves with a triexponential function (see also section 3.3 for further details):

$$y = A_1 \exp(-x/t_1) + A_2 \exp(-x/t_2) + A_3 \exp(-x/t_3) + y_0 \quad (2)$$

in order to optimize S/N ratio and by individuating on the fitting curves the point corresponding to half of the initial normalized amplitude ($\Delta A/2$) in whose correspondence $\tau_{1/2}$ is obtained. By applying the following equation pseudo-first order rate constants are calculated as follows:

$$k = (\tau_{1/2})^{-1} \quad (3)$$

$$k_{rec} = (\tau_{1/2})^{-1}_{blank} \quad (4)$$

$$k'_{reg} = (k - k_{rec}) \quad (5)$$

The following solutions were tested :

0.1 M LiOTf in acetonitrile (blank); 0.15 M 1, 0.1 M LiOTf , in acetonitrile (**1**): 0.15 M 3, 0.1 M LiOTf , in acetonitrile (**3**); 0.15 M 5, 0.1 M LiOTf , in acetonitrile (**5**); 0.15 M 7, 0.1 M LiOTf , in acetonitrile (**7**); 0.15 M 1,3-dimethylimidazolium iodide, 0.1 M LiI, in acetonitrile ($\mathbf{I^-}$); 0.15 M $[Co(bpy)_3](OTf)_2$, 0.1 M LiOTf , in acetonitrile (**Co(II)**).

3. Results and discussion

3.1 Optical spectroscopy

Optical features of complexes were studied by visible-NIR spectrophotometry. All copper(I) complexes appeared from light to dark red solids; coherently the absorption spectrum recorded in acetonitrile (Table 1) showed a broad band centred around 450 nm of intensity ca. $4.5 \cdot 10^3$ M^{-1} cm^{-1} attributed to a metal-to-ligand charge transfer transition (MLCT) [36]. The blue shift of complex **5**, contrary to expectation due to absence of any methyl group on the phenyl, points to a stronger hindrance [37] imposed by the aromatic substituents than in **1** and **3** analogues as a result, probably, of the free-rotation of the phenyl rings around the interanular bond (as confirmed by only three -Ph signals in ^{1}H-NMR) precluded to both tolyl and mesityl rings. The much higher molar absorption

coefficient for the unique alkyl substituted compound **7** resembles the trend observed for some 2,9-disubsituted analogues [38]. Interestingly, in **1** the absence of methyl groups in the 4,7 positions of phenanthroline determines a bathochromic shift of the absorption respect to the related compound $[Cu(2\text{-mesityl-4,7-dimethyl-1,10-phenantholine})_2]^+$. Moreover, the asymmetric substitution of the positions 2 and 9, in α of the coordinated nitrogen atoms, resulted in a less intense absorption if compared to the di-substituted benchmark compound $[Cu(2,9\text{-dimethyl-1,10-phenanthroline})_2]^+$, reducing the competitive absorption of light by the mediators respect to dyes. This observation further strengthens the assertion of a strict correlation between spectral intensity and symmetry of the complex, and hence the distortion from the tetrahedral geometry induced by ligand substituents [38]. Furthermore it suggests that ligand asymmetry decreases the intensity of MLCT bands regardless of whether it is introduced in 4,7 [38] or 2,9 positions.

Oxidized complexes invariably showed a broad band at around 690-750 nm attributed to a ligand field d-d transition (allowed by d^9 configuration of Cu atom) significantly less intense than the MLCT of copper(I) analogues (Table 1), eventually followed by a second weaker band at wavelengths around 900-1000 nm. These spectra are consistent with previous published analogues [29-31] and can be tentatively attributed to a five-coordinate geometry in solution, with acetonitrile as ancillary ligand of a trigonal bipyramide [39,40].

(Table 1)

3.2 Electrochemistry

Electrochemical behaviour of the copper-based coordination compounds were studied through cyclic voltammetry in acetonitrile. Concerning the anodic window (Figure 2), all complexes presented a single wave attributed to an electron transfer centred on the metal core, in agreement with literature [41], directly involved in both dye regeneration and cathodic reaction in DSSC operation. The process is perfectly chemically reversible and the superimposition of the pattern of a copper(I) compound with its oxidized counterpart is a clear proof of the mutual interconversion

between the two species. A peculiar situation occurred only for the copper(II) compound **2**, whose electron transfer mechanism seems to be more complicated, directly involving the solvent as already reported [31].

(Figure 2)

The oxidation potential of copper complexes (*i.e.* half-wave potential, $E_{1/2}$) is modulated by the nature of the 2-substituted-1,10-phenanthrolines through a combination of electronic and steric effects [41]. With respect to $E_{1/2}$ = –0.02 V *vs* $Fc^+|Fc$ of [Cu(2-mesityl-4,7-dimethyl-1,10-phenantholine)$_2$]$^+$ [29,30,41], complexes **1**-**8** exhibit positively shifted half-wave potentials ranging from 0.06 to 0.11 V *vs* $Fc^+|Fc$ (Table 2). Such anodic shift of the metal centered Cu(I)/(II) process can be reasonably attributed to the absence of electron rich methyl groups in 4,7 positions which increases the electron withdrawing properties of the aromatic ligands via dπ-π* bonding interactions. In a similar way, the progressive reduction of the number of $–CH_3$ on the 2-aryl moiety on going from **1** to **3** to **5** can be, at least partially, the reason for the $E_{1/2}$ positive shift. Nevertheless it is reasonable to take into account also the different steric hindrance and conformational rigidity of the substituents in position 2, which affect the geometry modification around the copper center, favouring or disfavouring a specific oxidation state of the copper atom and hence modulating both thermodynamic and kinetics of electron transfer. In fact, an important feature of d^{10} copper(I) complexes is a significant nuclear rearrangement due to the change of coordination geometry, from a tetrahedral to a tetragonal configuration upon oxidation to give d^9 copper(II) complexes [10]. However, steric constraints, such as the presence of sterically challenging groups in the α positions immediately adjacent to the coordinating nitrogen atoms of bipyridines or phenanthrolines, is an elegant way to control coordination geometry and its changes going from one oxidation state of the copper to the other [10]. In a similar way, the modulation of the inner-sphere reorganization energy of the complexes by substituents in position 2 regulates the rate of the electron transfer, according to the Marcus theory [42,43]. Table 2 summarizes the electron transfer rate constants, k_{heter},

obtained by Electrochemical Impedance Spectroscopy, EIS, measurements in acetonitrile on glassy carbon electrode. The heterogeneous rate constant was calculated according to $k_{heter} = \frac{RT}{F^2 C R_{ct} A}$, where R is the universal gas constant, T is the absolute temperature, F is the Faraday constant, C is the copper(I) complex concentration expressed in mol cm^{-3}, R_{ct} the charge transfer resistance at an applied bias equal to $E_{1/2}$ obtained by fitting EIS spectrum with the classical Randles circuit, and A the geometric area of the electrode in cm^{-2}. The fastest electron transfer occurred with **5**, k_{heter} $=1.9 \cdot 10^{-2}$ cm s^{-1} at $E_{1/2}$, comparable with the heterogeneous kinetics observed with the benchmark [Cu(2,9-dimethyl-1,10-phenanthroline)$_2$]$^+$ complex, while compound **7** with *n*-butyl chains on the ligands resulted to be the most sluggish of the series, with a three-times slower kinetics. A quantitative explanation that links structure of copper complexes, half-wave potential and electron transfer constant rate is out of the aim of the present work and will be carried out on a much larger series of complexes, where structure-activity relationships could be established with a better degree of certainty with respect to the small series herein presented. Nevertheless it is possible to note that the simple assertion relating higher half-wave potential to faster kinetic constant is not applicable, as exemplified by complex **7**. As observable from the relatively high value of $E_{1/2}$ of complex **7**, combined with its low k_{heter}, the alkyl substituents induce a geometry that well stabilizes the Cu(I) form but, at the same time, their flexibility (respect to the rigid planarity of aryl rings) does not efficiently hamper the geometry modification from Cu(I) to Cu(II) and vice versa, increasing the inner sphere reorganization energy, which ultimately turns into an higher activation barrier for the electron transfer. Among complexes **1**, **3**, **5** with 2-aryl substituted-1,10-phenanthrolines the rate constant increases with decreasing the number of methyl groups on the phenyl ring and so with reducing the steric hindrance of the substituents in position 2 while increasing their rotational freedom. For sake of comparison the heterogeneous rate constant of a cobalt(II) complex, [Co(bpy)$_3$]$^{2+}$ (bpy = 2,2'-bipyridine), was evaluated with the same protocol. Its value, $k_{heter}=8 \cdot 10^{-3}$ cm s^{-1}, is comparable with that of the two slowest copper(I) complexes, **1** and **7**.

(Table 2)

3.3 Dye regeneration

In a DSSC the reduced form of the mediator couple is tasked to react with the oxidized sensitizer, S^+, chemisorbed on the TiO_2 surface, in order to regenerate the starting form of the dye, S, as schematically depicted by the process (3) in Figure 1. Starting from some promising results [30, 32, 33] the fully-organic dye **G3** [32] was selected as a fruitful candidate to test the electron transfer properties of this new series. The capability of copper mediators to regenerate the sensitizer was evaluated by transient absorption spectroscopy (TAS), in comparison with reference donor species like $[Co(bpy)_3]^{2+}$ and I^-. In general, the oxidized dye recovery kinetics are described by a multiexponential behavior (like equation 2) essentially determined by the surface heterogeneity of the mesoscopic TiO_2 film, which results in a distribution of surface states from which recombination occurs with different rate constants. Due to this fact, recombination kinetics on TiO_2 have been described with the Kohlrausch William Watts (KWW) function (stretched exponential) by some authors [44]. In the absence of electron donors (blank electrolyte), oxidized dye recovery occurs only by recombination with the photoinjected electron (k_{rec}, equation 4) according to

$\mathbf{G3}^+ + e^-_{TiO2} \rightarrow \mathbf{G3}$

as schematically depicted by (6) in Figure 1.

Dye recovery kinetics monitored at 770 nm in a blank solution (*i.e.* acetonitrile with LiOTf) revealed a $\tau_{1/2,blank}$ around 56 μs (equation 4). Addition of electron donor species (**1**, **3**, **5**, **7**, $[Co(bpy)_3]^{2+}$, I^-) invariably reduces the lifetime, consistently with the electron transfer (k'_{reg}, equation 5) from the donor (D) to the oxidized dye (Figure 3) according to the competitive process depicted by (5) in Figure 1

$\mathbf{G3}^+ + D \rightarrow \mathbf{G3} + D^+$

Copper-based electron donors are characterized by a lower driving force for dye regeneration with respect to the two reference systems, namely cobalt (II) and iodide, being their oxidation half-wave

potential at least 120 mV and 340 mV more positive than $[Co(bpy)_3]^{2+}$ and I^-, respectively (using $E_{1/2}$ I^-/I_3^- = –0.28 V *vs* $Fc^+|Fc$, converted from 0.35 V *vs* NHE [33],[45]). Nevertheless, the kinetic competition between dye regeneration and recombination is in all cases favourable to a nearly quantitative regeneration efficiency (Table 3), expressed according to equation 2. All copper(I) complexes are able to assure regeneration of 50 % of the initial $\mathbf{G3}^+$ population chemisorbed on a transparent TiO_2 photoanode on a time interval varying between 0.7-2 μs, *i.e.* more than 20 times faster than the interfacial recombination. This implies regeneration efficiencies higher than 96% for the copper series, comparable or even higher than those obtained with cobalt (II) and I^- reference solutions (Table 3, where η ranges from 99% for **5** to 92% for I^-). Thus the differences in η, measured in the absence of applied forward bias, are always rather minor and should not cause significant variations in cell performance as long as dye regeneration is concerned. According to the semiclassical Marcus theory, the rate of electron transfer in a bimolecular reaction is given by the product of the electronic coupling, H_{AB}, proportional to the overlap between the wavefunctions of the electron donor and of the acceptor, with the nuclear activation term, where the Gibbs free energy of activation, $\Delta G^{\#}$, defined as $\Delta G^{\#} = \frac{(\lambda + \Delta G^0)^2}{4\lambda}$ appears. Within the copper series, both H_{AB} and the standard Gibbs free energy, ΔG^0, for each dye/copper donor are expected to be essentially constant (being $E_{1/2}$ of copper complexes very similar especially for **3**, **5**, **7**) while slight differences in the reorganization energy, λ, bearing the dominant contribution of the nuclear rearrangement that follows the Cu(I) →Cu(II) transition, probably contribute to explain the differences in the regeneration rate constant. Other more subtle factors, like local surface interactions between the mediator with the sensitized oxide surface and differences in the permeation of the titania mesopores by the liquid electrolyte may influence the outcome of regeneration rate constants.

Interestingly, it appears that the best pseudo first-order kinetic constant, k'_{reg}, is observed with complex **5** which also displays the highest heterogeneous electron transfer constant, k_{heter}, on glassy

carbon electrode. However developing a systematic correlation between the charge transfer kinetics observed at conventional working electrodes, like glassy carbon, and the regeneration rate observed at sensitized interfaces is difficult, and may lead to oversimplifications. Compared to glassy carbon, the polar surface of TiO_2 presents entirely different properties and the presence of a chemisorbed dye further adds to the interfacial complexity. Specific differences in the double layer structure between the two different electrodic materials and the specific electronic coupling which is established between the oxidized **G3** dye and the redox mediator are not taken into account in the voltammetric experiment at GC electrode. For example, in the case of the quasi-reversible cobalt (II)/(III) complexes, a large influence of the double layer structure on the heterogeneous charge transfer involving cobalt mediators has been reported [46] while modification of otherwise electrochemically inert substrates with certain molecular species was observed to promote a significant electrocatalysis towards the Co(II)/(III) couple [47,48]. A dependence of the electrochemical response on the nature of the electrodic material was also observed with both cobalt complexes [49] and some Cu(I)/(II) redox couples [29,30], suggesting also for the present case electrode-specific activation barriers for the heterogeneous electron transfer.

(Figure 3)

(Table 3)

3.4 Cu-complexes as electron mediators in DSSCs

Different electrolytes were prepared with each of the copper redox couples, dissolving 0.15 M of the copper(I) species (**1**, **3**, **5**, **7**) and 0.015 M of the corresponding copper(II) form (**2**, **4**, **6**, **8**) in acetonitrile. Essentially, 0.15 M concentration is close to the solubility limit for most of the copper complexes at RT in the solvent of our choice. Lithium trifluoromethanesulphonate (LiOTf) 0.1 M and *tert*-butylpyridine (tbp) 0.25 M were also added as additives in each formulation. For sake of comparison, reference electrolytes based on cobalt, $[Co(bpy)_3]^{2+/3+}$-El, and iodine/triiodine, I^-/I_3^--El,

were not optimized but prepared in identical way, *i.e.* equimolar concentration, with the same additives. This avoids spurious effects due to the mismatch in electrolyte composition and mediator concentration allowing to highlight the intrinsic impact of the properties of the various redox electrolytes on cell efficiency. Along with dye **G3** (PCE up to 8.6% with an optimized I^-/I_3^- electrolyte, under 100 mW cm^{-2} simulated AM 1.5G irradiation [32]) electrolytes were tested in solar devices sensitized with its analogue, **G4** (PCE up to 9.5% [33]), bringing one hexyl chain on the π–conjugated central scaffold with the aim to further hamper charge recombination by the oxidized mediator (Chart 1).

jE curves and related efficiency parameters for **G3**-sensitized DSSCs are reported in Figure 4 and Table 4, respectively.

(Figure 4)

(Table 4)

Impedance analysis performed at V_{oc} in the dark on **G3**-sensitized devices shows that differences in k_{heter} of copper complexes observed on the ideally inert GC electrode are partially equilibrated in DSSC, probably due to the quite different nature of the interfaces on which the electron transfer occurs, as previously discussed in section 3.3. In fact charge recombination (process (5) in Figure 1) for Cu-based mediators (*i.e.* the process occurring at medium frequencies, Figure 4) is characterized by comparable time constant of about 10 ms (equal to the inverse of the angular frequency at $-Z''_{max}$, Figure 4), similar to that of the control couple $[Co(bpy)_3]^{2+/3+}$. As a consequence photovoltages well correlate with the $E_{1/2}$ of the couples, *i.e.* the more positive is $E_{1/2}$ the higher is V_{oc}.

Interestingly most Cu-based redox couples are very efficient, outperforming **G3**-sensitized control cells filled with both I^-/I_3^- and $[Co(bpy)_3]^{2+/3+}$ reference electrolytes (prepared with comparable

concentrations). In particular, the slower charge recombination of I^-/I_3^--El (Figure 4) does not guarantee the highest open circuit potential, being negatively affected by the too negative $E_{1/2}$ of the couple with respect to copper complexes. The best performing redox couple **3**/**4** reached a 6.0% power conversion efficiency with both dyes, slightly improving the performance of our previous record couple **1**/**2** [31], mainly thanks to a 0.03-0.04 V improvement in V_{oc}. These two couples show similar electron transfer kinetics (Table 2) and comparable charge transfer recombination resistances (Figure 4) in DSSCs. This suggests that the improved performance of **3**/**4**–El with respect to **1**/**2**-El is related to lower overvoltage losses in the dye regeneration stage (due to its more positive oxidation potential), allowing to extract higher photovoltage while maintaining a nearly quantitative dye regeneration efficiency.

An anomaly in the **G3**-sensitized cells is **5**/**6**-El which is characterized by a quite low short circuit current density, which can be tentatively related to a poorer electron injection potentially attributable to an upshift of the TiO_2 conduction band edge energy. Such hypothesis would correlate well with the smaller drop in j_{sc} recorded with **G4** (Table 4), characterized by a ca. 0.1 eV higher LUMO energy than **G3** [33], which anyhow assures a good driving force for electron injection into the semiconductor. Another reason at the basis of the low photocurrent recorded with **5**/**6**-El may reside in a larger diffusional resistance of such redox couple, revealed in symmetric Pt/Pt cell (Figure 5).

(Figure 5)

In general, the Fill Factor of the **G3** sensitized cells varies between 59% and 69%. The highest value (69%) is observed with **5**/**6**-El, which however produces the lowest current. The cell Fill Factor is a measurement of the cell quality in terms of overvoltage losses in the cell, which can be expressed in the form of *jR* drops. The smaller these drops are, the better is *FF*. In particular, *R* is the sum of all the serial resistances of the cell, including ohmic, charge transfer and mass transport

resistances. It is not surprising that the best Fill Factor is thus observed in the presence **5**/**6**-El, endowed with a ca. 30% lower photocurrent with respect to the best couples, since the *jR* drop scales with the photocurrent. In our case, the best compromise is found with **3**/**4**-El and **7**/**8**-El for which *FF* is still 62 and 66% respectively, while the photocurrent is at least 20% higher than **5**/**6**-El. Contrary to what previously reported for optimized I^-/I_3^--El [33], the introduction of hexyl chain along the π-conjugated backbone of the **G4** dye does not bring the expected positive effects on the recombination by Cu-based electrolytes. In fact PCEs remain equal (**3**/**4**-El) or even slightly lower (in all the other cases) than with the simpler **G3** sensitizer (Table 4), essentially due to a lower photovoltage. In the case of **5**/**6**-El the increased j_{sc} is offset by a decreased photovoltage and *FF*, and the resulting PCE is essentially the same, but in the case of **7**/**8**-El the drop in photovoltage (0.08 V) and slightly reduced *FF* (63% for **G4** *vs* 66% for **G3**) pairs with an unchanged photocurrent density (10.1 mA cm^{-2}). The lower V_{oc} generally observed with **G4** could be reasonably explained by a faster charge recombination involving copper(II) complexes on the titania surface.

4. Conclusions

Four Cu^+/Cu^{2+} redox couples constituted by homoleptic complexes of 2-substituted-1,10-phenanthrolines were synthesized. Functionalization of the positions adjacent to nitrogen atoms allows to modulate both optical and electrochemical features of the related copper complexes. As a result, combination of visible absorption spectroscopy and cyclic voltammetry shows that the asymmetric substitution of ligands (*i.e.* functionalization of internal position 2) is an elegant way to produce copper-based redox couples with valuable features as electron mediators in dye-sensitized solar cells. In particular 2-subsituted ligands decrease intensity of the MLCT bands of related Cu(I) coordination compounds, resembling the already known effect of the asymmetry induced by the 4,7 external positions of phenanthrolines. This effect is amplified if aryl groups are preferred to alkyl ones. The electrochemical study reveals that $E_{1/2}$ and k_{heter} are not directly proportional, but they are

influenced by the geometry of the complex and by its flexibility, which are modulated not only by the steric hindrance but also by the rotational freedom of the internal substituents.

As a result 2-aryl derivatives effectively combine optimal optical and electrochemical properties, thanks to lower molar extinction coefficients, sufficiently positive oxidation potentials and well-balanced electron transfer kinetics resulting in nearly quantitative dye regeneration efficiencies under short circuit conditions. While the details of the mechanistic correlation between synthetic design, basic electrochemical properties, and the resulting power conversion in the solar devices remained elusive, due to the presence of different complex interfaces and the interlacing of several processes involved in cell functioning, it can be affirmed that the proposed synthetic design was generally successful in producing mediators endowed with a reduced overvoltage loss associated to the dye regeneration process. As a result **3**/**4**-El neatly shows a 20% and 15% increase in PCE respect to the common $[Co(bpy)_3]^{2+/3+}$ and I^-/I_3^- couples, respectively, formulated at comparable concentration, overcoming also our previous best performing copper-based mediator, **1**/**2**-El, thanks to a more positive half-wave potential.

The extension of these studies to a wider Cu(I)/(II) series, the back up by DFT calculations, as well as the examination of the dye regeneration kinetics in the working device under applied bias are expected to bring a clearer correlation between the basic optical and electrochemical properties of these species with cell performance, paving the way towards a further generation of optimized copper-based mediators.

Acknowledgements

A. C. thanks Università degli Studi di Milano (Piano Sostegno alla Ricerca 2015–17-LINEA 2 Azione A – Giovani Ricercatori) for financial support. R.G. and G.P.S. acknowledge funding from the Austrian Research Promotion Agency-FFG (Bridge-Early Stage COMPOSTRONICS cod. 5730587). The “Ministero degli Affari Esteri e della Cooperazione Internazionale” (bilateral project

Italy-India, Prot. nr. MAE0104617) is also acknowledged for financial support. We thank both Regione Lombardia and Fondazione Cariplo for the use of instrumentation purchased through the SmartMatLab Centre project (2014). POR-FESR HP Solar and Solarchem are gratefully acknowledged (UNIFE).

References

[1] *Dye-sensitized Solar Cells,* ed K. Kalyanasundaram, EPFL Press, Lausanne, 2010.

[2] Global Dye-sensitized Solar Cells (DSSC) Market Professional Survey 2016 Industry Trend and Forecast 2021, QY Research (2016).

[3] A. Fakharuddin, R. Jose, T.M. Brown, F. Fabregat-Santiago, J. Bisquert, A perspective on the production of dye-sensitized solar modules. Energy Environ. Sci., 7 (2014), pp. 3952-398.

[4] B. O'Regan, M. Grätzel, A low-cost, high-efficiency solar cell based on dye-sensitized colloidal TiO_2 films, Nature 353 (1991) 737–740.

[5] M. Grätzel, Recent Advances in Sensitized Mesoscopic Solar Cells. Accounts Chem. Res., 42 (2009) 1788-1798.

[6] G. C. Vougioukalakis, A. I. Philippopoulos, T. Stergiopoulos , P. Falaras, Contributions to the development of ruthenium-based sensitizers for dye-sensitized solar cells, Coord. Chem. Rev. 255 (2011) 2602-2621.

[7] L.-L. Li and E. W.-G. Diau, Porphyrin-sensitized solar cells, Chem. Soc. Rev. 42 (2013) 291-304.

[8] C. E. Housecroft, E. C. Constable, The emergence of copper(I)-based dye sensitized solar cells, Chem. Soc. Rev. 44 (2015) 8386-8389.

[9] M. Sandroni, Y. Pellegrin and F. Odobel, Heteroleptic bis-diimine copper(I) complexes for applications in solar energy conversion, C. R. Chimie 19 (2016) 79-93.

[10] M. Magni, P. Biagini, A. Colombo, C. Dragonetti, D. Roberto, A. Valore, Versatile copper complexes as a convenient springboard for both dyes and redox mediators in dye sensitized solar cells, Coord. Chem. Rev. 322 (2016) 69–93.

[11] C.-Y. Chen, M. Wang, J.-Y. Li, N. Pootrakulchote, L. Alibabaei, C. Ngoc-le, J.-D. Decoppet, H.-H. Tsa, C. Graetzel, C.-G. Wu, S. M. Zakeeruddin, M. Graezel, Highly Efficient Light-Harvesting Ruthenium Sensitizer for Thin-Film Dye-Sensitized Solar Cells, ACS Nano 3 (2009) 3103-3109.

[12] Q. Yu, Y. Wang, Z. Yi, N. Zu, J. Zhang, M. Zhang and P. Wang, High-Efficiency Dye-Sensitized Solar Cells: The Influence of Lithium Ions on Exciton Dissociation, Charge Recombination, and Surface States, ACS Nano 4 (2010) 6032-6038.

[13] H. Ozawa, Y. Okuyama and H. Arakawa, Dependence of the efficiency improvement of black-dye-based dye-sensitized solar cells on alkyl chain length of quaternary ammonium cations in electrolyte solutions, ChemPhysChem, 15 (2014) 1201-1206.

[14] C.A. Bignozzi, R. Argazzi, R. Boaretto, E. Busatto, S. Carli, F. Ronconi, S. Caramori, The role of transition metal complexes in dye sensitized solar devices, Coord. Chem. Rev. 257 (2013) 1472–1492.

[15] B. Pashaei, H. Shahroosvand, P. Abbasi, Transition metal complex redox shuttles for dye-sensitized solar cells, RSC Adv. 5 (2015) 94814–94848.

[16] T.W. Hamann, The end of iodide? Cobalt complex redox shuttles in DSSCs, Dalton Trans. 41 (2012) 3111-3115.

[17] L. Giribabu, R. Bolligarla, M. Panigrahi, Recent Advances of Cobalt(II/III) Redox Couples for Dye-Sensitized Solar Cell Applications, Chem. Rec. 15 (2015) 760–788.

[18] A. Yella, H.-W. Lee, H. N. Tsao, C. Yi, A. K. Chandiran, Md. K. Nazeeruddin, E. W.-G. Diau, C.-Y. Yeh, S. M. Zakeeruddin, M. Graetzel, Porphyrin-sensitized solar cells with cobalt (II/III)-based redox electrolyte exceed 12 percent efficiency, Science 334 (2011) 629-634.

[19] S. Mathew, A. Yella, P. Gao, R. Humphry-Baker, B. F. E. Curchod, N. Ashari-Astani, I. Tavernelli, U. Rothlisberger, M. K. Nazeeruddin, M. Grätzel, Dye-sensitized solar cells with 13% efficiency achieved through the molecular engineering of porphyrin sensitizers, Nature Chemistry, 6 (2014) 242-247.

[20] K. Kakiage, Y. Aoyama, T. Yano, K. Oya, J. Fujisawa, M. Hanaya, Highly-efficient dye-sensitized solar cells with collaborative sensitization by silyl-anchor and carboxy-anchor dyes, Chem. Commun. 51 (2015) 15894–15897.

[21] L. Kavan, Y.Saygili, M. Freitag, S.M. Zakeeruddin, A. Hagfeldt, M. Grätzel, Electrochemical properties of Cu(II/I)-based redox mediators for dye-sensitized solar cells. Electrochim. Acta 227 (2017) 194-202.

[22] S. Hattori, Y. Wada, S. Yanagida, S. Fukuzumi, Blue Copper Model Complexes with Distorted Tetragonal Geometry Acting as Effective Electron-Transfer Mediators in Dye-Sensitized Solar Cells, J. Am. Chem. Soc. 127 (2005) 9648–9654.

[23] Y. Bai, Q. Yu, N. Cai, Y. Wang, M. Zhang, P. Wang, High-efficiency organic dye-sensitized mesoscopic solar cells with a copper redox shuttle, Chem. Commun. 47 (2011) 4376–4378.

[24] M. Freitag, F. Giordano, W. Yang, M. Pazoki, Y. Hao, B. Zietz, M. Graetzel, A. Hagfeldt, G. Boschloo, Copper Phenanthroline as a Fast and High-Performance Redox Mediator for Dye-Sensitized Solar Cells, J. Phys. Chem. C 120 (2016) 9595−9603.

[25] Y. Saygili, M. Söderberg, N. Pellet, F. Giordano, Y. Cao, A. Belen Muñoz-García, S. M. Zakeeruddin, N. Vlachopoulos, M. Pavone, G. Boschloo, L. Kavan, J.-E. Moser, M. Graetzel, A. Hagfeldt, M. Freitag, Copper Bipyridyl Redox Mediators for Dye-Sensitized Solar Cells with High Photovoltage, J. Am. Chem. Soc. 138 (2016) 15087−15096.

[26] J. Cong, D. Kinschel, Q. Daniel, M. Safdari, E. Gabrielsson, H. Chen, P. H. Svensson, L. Sun, L. Kloo, Bis(1,1-bis(2-pyridyl)ethane)copper(I/II) as an efficient redox couple for liquid dye-sensitized solar cells, J. Mater. Chem. A 4 (2016) 14550–14554.

[27] J. Li, X. Yang, Z. Yu, G. G. Gurzadyan, M. Cheng, F. Zhang, J. Cong, W. Wang, H. Wang, X. Li, L. Kloo, M.Wang, L. Sun, Efficient dye-sensitized solar cells with [copper(6,6′-dimethyl-2,2′-bipyridine)$_2$]$^{2+/1+}$ redox shuttle, RSC Adv. 7 (2017) 4611–4615.

[28] M. Freitag, J. Teuscher, Y. Saygili, X. Zhang, F. Giordano, P. Liska, J. Hua, S.M. Zakeeruddin, J.-E. Moser, M. Grätzel, A. Hagfeldt, Dye-sensitized solar cells for efficient power generation under ambient lighting, Nat. Photonics 11 (2017) 372−378.

[29] A. Colombo, C. Dragonetti, M. Magni, D. Roberto, F. Demartin, S. Caramori, C.A. Bignozzi, Efficient Copper Mediators Based on Bulky Asymmetric Phenanthrolines for DSSCs, ACS Appl. Mater. Interfaces 6 (2014) 13945–13955.

[30] M. Magni, R. Giannuzzi, A. Colombo, M. P. Cipolla, C. Dragonetti, S. Caramori, S. Carli, R. Grisorio, G. P. Suranna, C. A. Bignozzi, D. Roberto, M. Manca, Tetracoordinated Bis-phenanthroline Copper-Complex Couple as Efficient Redox Mediators for Dye Solar Cells, Inorg. Chem. 55 (2016) 5245−5253.

[31] A. Colombo, G. Di Carlo, C. Dragonetti, M. Magni, A. Orbelli Biroli, M. Pizzotti, D. Roberto, F. Tessore, E. Benazzi, C. A. Bignozzi, L. Casarin, S. Caramori, Coupling of Zinc Porphyrin Dyes and Copper Electrolytes: A Springboard for Novel Sustainable Dye-Sensitized Solar Cells, Inorg. Chem. 56 (2017) 14189−14197.

[32] R. Grisorio, L. De Marco, C. Baldisserri, F. Martina, M. Serantoni, G. Gigli, G. P. Suranna, Sustainability of Organic Dye-Sensitized Solar Cells: The Role of Chemical Synthesis, ACS Sustainable Chem. Eng., 3 (2015) 770–777.

[33] R. Grisorio, L, De Marco, R. Giannuzzi, G. Gigli, G. P. Suranna, Molecular engineering of largely π-extended metal-free sensitizers containing benzothiadiazole units: Approaching 10% efficiency dye-sensitized solar cells using iodine-based electrolytes, Dyes and Pigments, 131 (2016) 282–292.

[34] W. Sharmoukh, A. Attanzio, E. Busatto, T. Etienne, S. Carli, A. Monari, X. Assfeld, M. Beley, S. Caramori, P.C. Gros, 2,5-Dithienylpyrrole (DTP) as a donor component in DTP–π–A organic sensitizers: photophysical and photovoltaic properties, RSC Adv. 5 (2015) 4041−4050.

[35] J.-H. Yum, E. Baranoff, F. Kessler, T. Moehl, S. Ahmad, T. Bessho, A. Marchioro, E. Ghadiri, J.-E. Moser, C.Yi, M.K. Nazeeruddin, M. Grätzel, A cobalt complex redox shuttle for dye-sensitized solar cells with high open-circuit potentials, Nature Commun. 3 (2012) 361.

[36] A. K. Ichinaga, J. R. Kirchhoff, D. R. McMillin, C. O. Dietrich-Buchecker, P. A. Marnot, J.-P. Sauvage, Charge-transfer absorption and emission of $Cu(NN)_2^+$ systems, Inorg. Chem., 26 (1987) 4290–4292.

[37] N. A. Gothard, M. W. Mara, J. Huang, J. M. Szarko, B. Rolczynski, J. V. Lockard, L. X. Chen, Strong Steric Hindrance Effect on Excited State Structural Dynamics of Cu(I) Diimine Complexes, J. Phys. Chem. A, 116 (116) 1984−1992.

[38] N. Armaroli, Photoactive mono- and polynuclear Cu(I)–phenanthrolines. A viable alternative to Ru(II)–polypyridines?, Chem. Soc. Rev., 30 (2001) 113−124.

[39] Y. Yao, M. W. Perkovic, D. P. Rillema, C. Woods, C., Structures and Properties of Copper(II) and Copper(I) Complexes Containing an Ethane-Bridged Dimeric Phenanthroline Ligand, Inorg. Chem., 31 (1992) 3956-3962.

[40] Md. A. Masood, D. J. Hodgson, Synthesis and Characterization of the Multidentate Ligand 2,9-Bis(N-pyrazolylmethyl)-l,10-phenanthroline (bpmp) and Its Copper(I) and Copper(II) Complexes, Inorg. Chem., 32 (1993) 4839-4844.

[41] M. Magni, A. Colombo, C. Dragonetti, P. Mussini, Steric vs electronic effects and solvent coordination in the electrochemistry of phenanthroline-based copper complexes, Electrochimica Acta, 141 (2014) 324–330.

[42] R. A. Marcus, On the Theory of Oxidation-Reduction Reactions Involving Electron Transfer. J. Chem. Phys., 24 (1956) 966–978.

[43] R. A. Marcus, On the Theory of Electron-Transfer Reactions. VI. Unified Treatment for Homogeneous and Electrode Reactions, J. Chem. Phys., 43 (1965) 679–701.

[44] L. Casarin, W.B. Swords, S. Caramori, C.A. Bignozzi, G. J. Meyer, Rapid Static Sensitizer Regeneration Enabled by Ion Pairing, Inorg. Chem. 56 (2017) 7324-7327.

[45] J. G. Rowley, By. H. Farnum, S. Ardo, G. J. Meyer, Iodide Chemistry in Dye-Sensitized Solar Cells: Making and Breaking I−I Bonds for Solar Energy Conversion, J. Phys. Chem. Lett., 1 (2010) 3132-3140.

[46] R. S. Gaddie, C. B. Moss, C. M. Elliott, Cyclic Voltammetric Study of Cobalt Poly-4-t-butylpyridine Ligand Complexes on Glassy Carbon Electrodes: Electrolyte Dependence and Mechanistic Considerations, Langmuir 29 (2013) 825-831.

[47] C. M. Elliott, S. Caramori, C. A. Bignozzi, Indium Tin Oxide Electrodes Modified with Tris(2,2’-bipyridine-4,4’-dicarboxylic acid) Iron(II) and the Catalytic Oxidation of Tris(4,4’-di-tert-butyl-2,2‘-bipyridine) Cobalt(II), Langmuir 21 (2005) 3022-3027.

[48] M. J. Scott, J. J. Nelson, S. Caramori, C. A. Bignozzi, C. M. Elliott, cis-Dichloro-bis(4,41-dicarboxy-2,2-bipyridine)osmium(II)-Modified Optically Transparent Electrodes: Application as Cathodes in Stacked Dye-Sensitized Solar Cells, Inorg. Chem. 46 (2007) 10071-1078.

[49] S. Carli, L. Casarin, Z. Syrgiannis, R. Boaretto, E. Benazzi, S. Caramori, M. Prato, C. A. Bignozzi, Single Walled Carbon Nanohorns as Catalytic Counter Electrodes for Co(III)/(II) Electron Mediators in Dye Sensitized Cells, ACS Appl. Mater. Interfaces 8 (2016) 14604-14612.

Table 1 Electronic absorption parameters (maximum absorption wavelength, λ_{max}, and related molar absorption coefficient (ε) for copper(I) and copper(II) complexes dissolved in acetonitrile.

Compound		λ_{max} /nm (10^3 ε /$M^{-1}cm^{-1}$)
copper(I)	**1**	451 (4.2)
	3	455 (4.6)
	5	437 (4.6)
	7	452 (6.2)
	[Cu(2-mesityl-4,7-dimethyl-1,10-phenantholine)$_2$]$^{+}$ [a]	445 (4.4)
	[Cu(2,9-dimethyl-1,10-phenanthroline)$_2$]$^{+}$ [a]	455 (8.0)
copper(II)	**2**	695 (0.124)
	4	688 (0.079)
	6	691 (0.113)
	8	756 (0.096)

[a] See references 29 and 30.

Table 2 Electrochemical parameters (half-wave potential, $E_{1/2}$, and rate constant, k_{heter}, at $E_{1/2}$) for complexes discussed in the text. [a]

Compound	$E_{1/2}$ *vs* Fc^+/Fc /V	$10^3 k_{heter}$ /cm s^{-1} [b]
$[Cu(2\text{-mesityl-}4,7\text{-dimethyl-}1,10\text{-phenantholine})_2]^+$ [c]	–0.02	7±1
1	0.06	9.1±0.1
3	0.09	11±1
5	0.10	19±4
7	0.11	6±1
$[Cu(2,9\text{-dimethyl-}1,10\text{-phenanthroline})_2]^+$ [c]	0.30	20±2
$[Co(bpy)_3]^{2+}$	–0.06	8±1

[a] Recorded on glassy carbon electrode, $1 \cdot 10^{-3}$ M in acetonitrile with $TBAPF_6$ 0.1M.
[b] Average of at least two independent measurements. Temperature 297±2 K.
[c] See references 29 and 30.

Table 3 Main parameters obtained by fitting dye recovery traces of Figure 3.

	$\tau_{1/2}$ /s	k'_{reg} /s^{-1}	η_{reg}
1	2.3E-06	4.2E+05	0.96
3	8.1E-07	1.2E+06	0.99
5	6.7E-07	1.5E+06	0.99
7	1.5E-06	6.5E+05	0.97
$[Co(bpy)_3]^{2+}$	2.5E-06	2.8E+05	0.96
I^-	4.4E-06	2.1E+05	0.92

Table 4 Photoelectrochemical parameters for **G3-** and **G4-** (in parenthesis) sensitized solar cells filled with Cu-based electrolytes (area=0.14 cm^2). For sake of comparison control cells filled with $[Co(bpy)_3]^{2+/3+}$-El and I^-/I_3^--El at comparable concentrations are also reported. Irradiation =100 mW cm^{-2} simulated AM 1.5G.

Electrolyte	***PCE* %**[a]	***FF***[b]	V_{oc} /V	j_{sc} /mA cm^{-2}
1/2-El	5.6 (5.3)	0.59 (0.54)	0.83 (0.84)	11.4 (11.7)
3/4-El	6.0 (6.0)	0.62 (0.62)	0.87 (0.87)	11.1 (11.1)
5/6-El	4.9 (4.8)	0.69 (0.58)	0.88 (0.81)	8.0 (10.2)
7/8-El	5.7 (4.9)	0.66 (0.63)	0.86 (0.78)	10.1 (10.1)
$[Co(bpy)_3]^{2+/3+}$-El	4.7	0.68	0.79	8.8
I^-/I_3^--El	5.2	0.59	0.71	12.6

[a] photon-to-current conversion efficiency. [b] Fill factor.

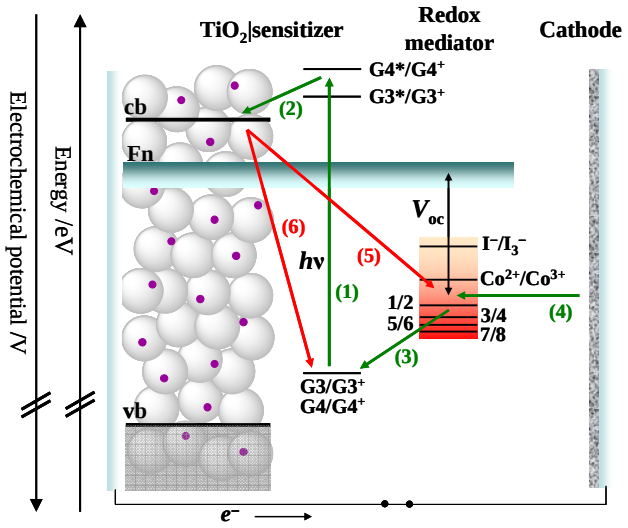

Figure 1. Qualitative energetic scheme of a DSSC employing sensitizers and redox mediators studied in this paper. Vb and cb stands for valence and conduction band of TiO_2, respectively; Fn represent the quasi-Fermi level of electrons in TiO_2; V_{oc} is the open circuit potential under irradiation. Green arrows depict the operative pathway, including photoexcitation of the sensitizer (1), electron injection into cb of TiO_2 (2), dye regeneration (3), mediator regeneration at cathode (4). Red arrows represent undesired charge recombination processes by oxidized form of the redox couple in solution (5) and of the chemisorbed dye (6).

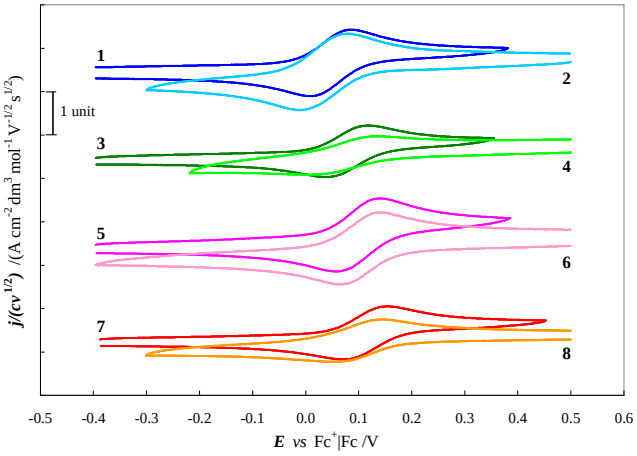

Figure 2 Cyclovoltammograms (0.2 V s^{-1}, glassy carbon electrode) of the cuprous (odd numbers) and cupric (even numbers) form of the four redox couples. Working medium: acetonitrile with [TBA]PF_6 0.1M. Pattern of compound **2** was obtained after addition of a small excess of ascorbic acid.

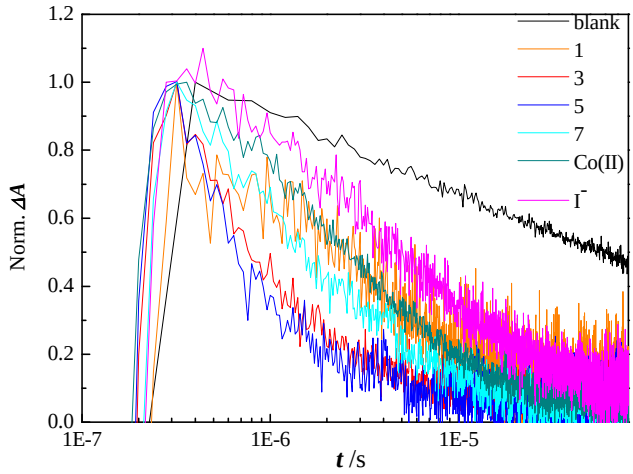

Figure 3 Dye recovery traces at 770 nm of **G3** chemisorbed on transparent TiO_2 substrate.

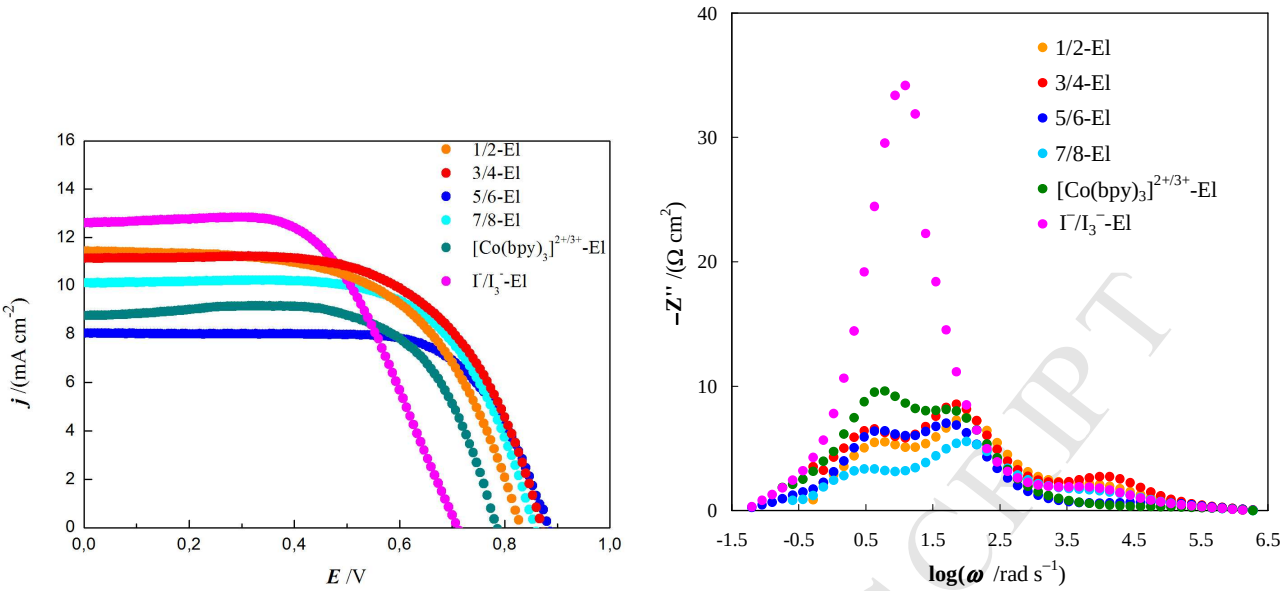

Figure 4 Left: *jE* curves for **G3**-sensitized DSSCs. Right: imaginary impedance plots recorded at V_{oc} in dark.

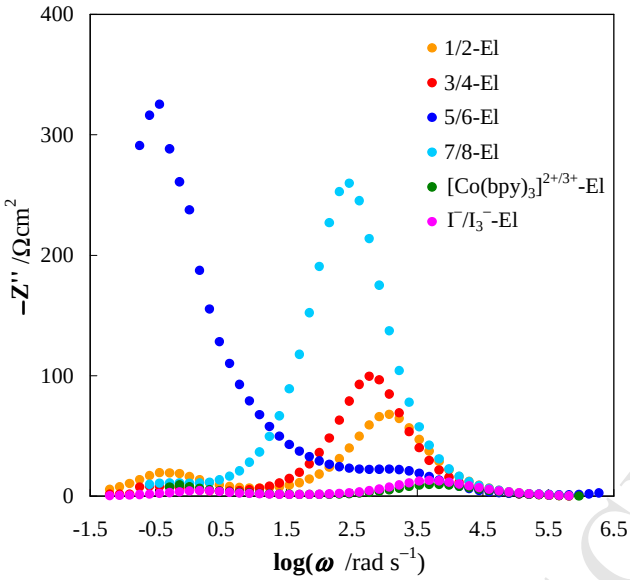

Figure 5 Imaginary impedance plots (E_{bias} = 0 V) for symmetrical Pt|electrolyte|Pt cells.

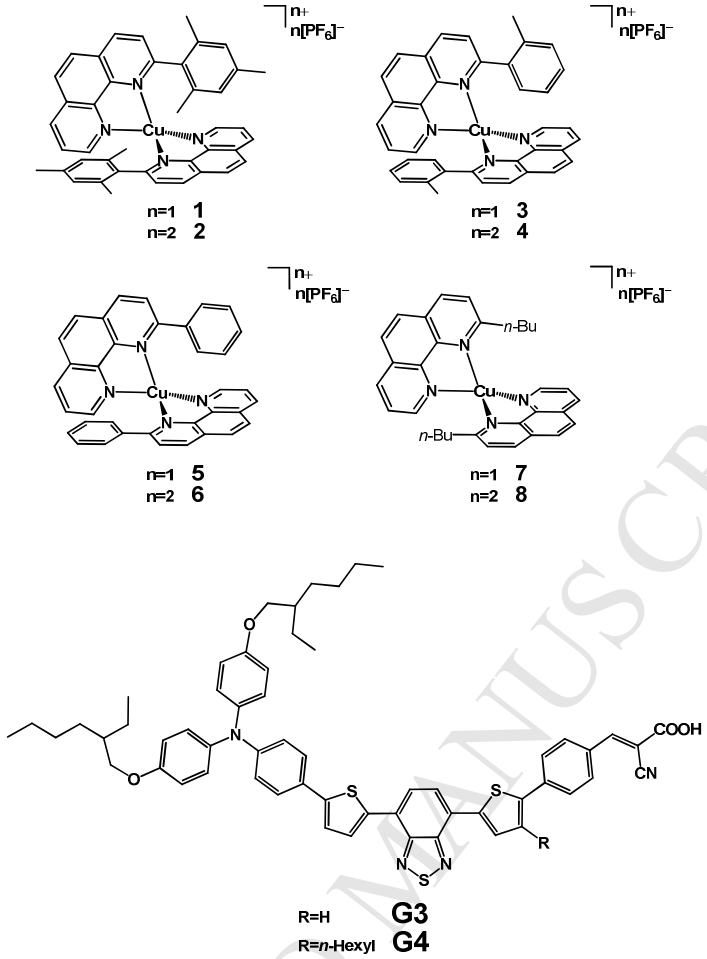

Chart 1 Molecular structure of the copper complexes employed as redox mediators, **1**-**8**, and of the metal-free dyes employed for sensitization of TiO_2 photoanode of DSSCs, **G3** and **G4**.

Highlights:

- Copper complexes with tunable redox potentials and electron transfer kinetics;
- Correlation between ligand substituents, electrochemical features and DSSCs output;
- Efficient redox mediators overcoming cobalt- and iodine-based reference couples, under comparable conditions